Small-Angle Charge-Exchange Scattering of He^+ by He, Ne, and Kr at Energies between 1.00 and 3.00 keV*†

Stephen W. Nagy,‡ Salvador M. Fernandez, and Edward Pollack
Physics Department, University of Connecticut, Storrs, Connecticut 06268
(Received 8 June 1970)

The scattering of He^+ by He, Ne, and Kr is studied in the energy range 1.00–3.00 keV and in an angular region from 0° to about 3°. These studies yield information on the probability of charge exchange P_0 as a function of beam energy and scattering angle. For the $He^+ + He$ case, the positions of the maxima and minima of P_0 generally agree with those of previous experiments. A wider range of P_0 values is obtained, however, and the current results lend more credence to a two-state resonant-charge-exchange theory for the $He^+ + He$ collision. In the $He^+ + Ne$ collision, the charge-exchange differential cross section is found to increase with increasing energy, while the non-charge-exchange differential cross section decreases. An unexpected result of the current studies on Ne is that the positions of the maxima and minima of the scattered neutral He (and of P_0) are independent of energy. These results are not consistent with a curve-crossing model for the charge-exchange process, which predicts an angular structure dependent on energy. Studies of the $He^+ + Kr$ collision show a broad forward He peak with no pronounced structure in the energy and angular region investigated.

I. INTRODUCTION

In recent years, a great deal of experimental and theoretical effort has gone into studies of collisions between ions and atoms which result in charge exchange between the collision partners. While elastic processes are generally well understood, relatively few inelastic processes are easily explained by theory. More specifically, no theory has yet been developed which explains both elastic and inelastic charge-exchange processes. Since both types are easily observable in the laboratory, the wealth of information available from experimental measurements may serve to guide the development of a more comprehensive theory. Furthermore, a better understanding of the charge-exchange process is important in view of its role in plasma physics as well as in upper atmospheric phenomena.

By far the greatest number of charge-exchange studies have been concerned with the energy dependence of the total cross section. Even for this relatively simple class of experiments, there is a good deal of disagreement between the results of different laboratories as well as between the results of different theoretical groups. Although a comparison of experimental with theoretical total cross sections is often used to test the validity of the theory, a more definitive test results from a comparison of differential cross sections, or from a comparison of the angular distributions of the scattered particles.

This paper investigates three types of charge exchange: resonant in $He^+ + He$, quasiresonant in $He^+ + Ne$, and apparently nonresonant in $He^+ + Kr$. All the measurements are made at laboratory scattering angles of less than 3° and in the energy range 1.00–3.00 keV. A relatively high angular resolution is obtained by exclusive use of collimating holes rather than of slits or combinations of slits and holes. Measurements are made directly on the neutral atoms resulting from charge exchange as well as on the combined neutral and ion beams. The scattered neutral atoms are studied even in forward scattering, since it is possible to distinguish them from the incident ions.

The experimental results for P_0, the probability of charge exchange, as a function of angle in the $He^+ + He$ case generally compare favorably with previous work as far as the locations of the maxima and minima are concerned. However, the minima reported here generally exhibit lower values and the maxima higher values than those of the earlier work. The wider range in P_0 values in the present experiment is primarily due to increased angular resolution, and lends more credence to a two-state resonant-charge-exchange theory for the $He^+ + He$ case. The $He^+ + Ne$ results show P_0 to depend only on angle and not on energy in the region studied. The angular distributions of the neutral atoms are peaked in the forward direction and exhibit a marked oscillatory structure. The $He^+ + Kr$ results show a forward peak and a monotonic decrease with increasing angle in the neutral beam intensity.

The high-resolution data obtained in the $He^+ + He$ collision suggest a novel experimental technique for comparing the detection efficiency of a neutral atom to the corresponding ion. It is well known that in resonant charge exchange, such as in $He^+ + He$, the intensity of the scattered neutral (He) beam exhibits a marked oscillatory structure when plotted as a function of angle. A similar structure, differing in phase, is obtained for the ion (He^+) signal. Assuming negligible contributions from inelastic channels, the combined ion and neutral beam intensities should decrease monotonically with increasing angle. An oscillatory structure will result in the combined sig-

nal when the detection efficiencies of the neutral atom and ion are different. As an example at those angles where the neutral signal predominates, a low relative detection efficiency for neutral atoms would result in a signal which falls below the expected smooth curve. The suggested technique involves a high-angular-resolution measurement of the combined neutral and ion beam intensities as a function of angle. The envelopes of the maxima (where the ions predominate) and minima (where the neutral atoms predominate) are compared and yield the ratio of detection efficiencies.

II. APPARATUS

As Fig. 1 shows, the apparatus consists basically of three vacuum chambers: the source, the scattering, and the detector chambers.

The source chamber is the largest of the three and houses the ion source, the mass analyzer and the ion optics systems, and a support tube for two buttons containing beam collimation holes. This chamber is mounted on a circular stainless-steel table and is pumped by a 6-in. diffusion pump. A cold trap mounted above this diffusion pump is maintained at a temperature of $-50\ ^{\circ}C$ by a refrigeration system. With the ion source in operation, the pressure maintained in this chamber is about 1×10^{-6} Torr. The ion source, mass analyzer, and the ion optics system are described in a previous paper.[1] The collimation holes, F and G in Fig. 1, are both of 0.005 in. diam and are separated by 4.313 in. This results in a minimum geometrical angular resolution of 0.062° for the incident He^{+} beam. The use of holes rather than slits is dictated by the requirement that the data taken at small angles be of high angular resolution.

The scattering chamber, also shown in Fig. 1, is constructed from solid brass and is entirely gold plated. It is bolted to the source chamber and is attached to the detector chamber via a flexible stainless-steel bellows. Ultrapure helium (ionization grade), neon, and krypton are supplied to this region by means of a precision leak valve. The scattering chamber is also connected to a ballast tank to minimize pressure fluctuations during a run. Connected to the ballast tank is a liquid-nitrogen cold trap and a 2-in. diffusion pump. The pressure in this system, as monitored by a Bayard-Alpert-type ionization gauge, is generally 7×10^{-8} Torr before the introduction of the target gas. Positioned at the top of the scattering chamber is a feedthrough, to which an electrically isolated Faraday cup is attached. This Faraday cup is used to monitor the incident ion beam and is moved out of the beam path whenever it is not in use.

The detector chamber, like the source chamber, is mounted on the circular table and rotates about the axis of a precision stainless-steel-sleeve bearing. The axis of this bearing intercepts the scattering center, and thus the detector chamber is constrained to rotate about this center. Contained in this chamber are the detector collimation holes which define the angular resolution of the detected beam, an electrostatic analyzer, and a secondary electron multiplier. The vacuum in this chamber is generally below 4×10^{-7} Torr. This is attained through the use of a 4-in. diffusion pump with the aid of a cold trap, refrigerated to $-40\ ^{\circ}C$, mounted above it.

Although the collision occurs in the scattering

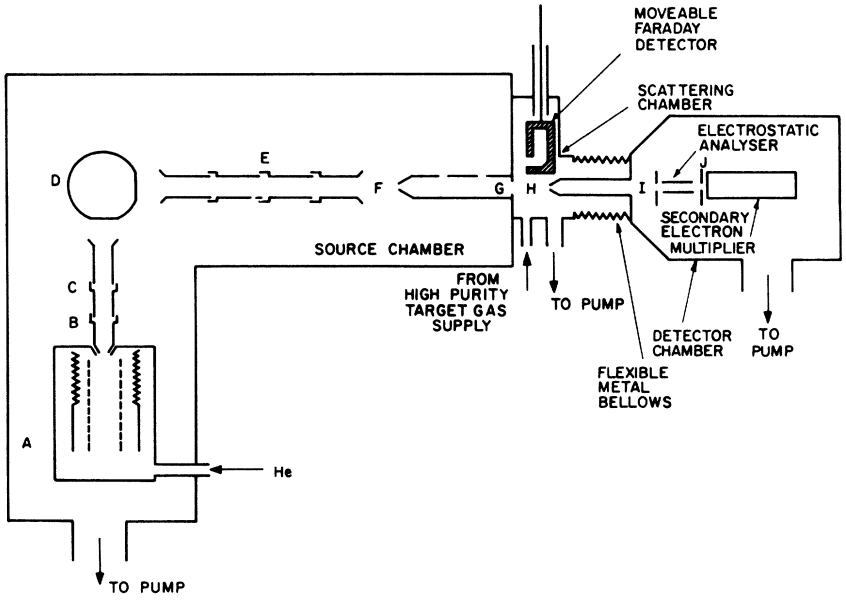

FIG. 1. Schematic diagram of the apparatus. (A) ion source; (B) extractor; (C) ion optics; (D) mass-analyzer magnet; (E) ion optics; (F), (G), (H), and (I) collimating holes; (J) slit.

chamber, the scattering length varies with the angular orientation of the detector. When the angle between the incident beam path and detector is 0°, the on-axis distance between G and H is 0.625 in. H and I are circular 0.005-in.-diam holes separated by 4.125 in., and being attached to the detector chamber serve to define the angular position of the scattered signal. The minimum geometrical angular resolution of this pair of holes is 0.073°. The worst angular resolution of the apparatus is 0.135° and is obtained as the sum of the minimum angular resolutions of the two pairs of holes F-G and H-I.

Once the scattered particles pass through the final collimation hole, they are charge-state analyzed by an electrostatic analyzer. A horizontal slit, labeled J in Fig. 1, is mounted directly in front of an I. T. T. F-141 secondary electron multiplier. Both the slit and multiplier are mounted on a spring-loaded multiplier support (not shown in Fig. 1) which is free to rotate in a vertical plane about a horizontal line centered between the electrostatic analyzer plates. The secondary electron multiplier followed by digital electronics count the particles striking the first dynode of the multiplier.

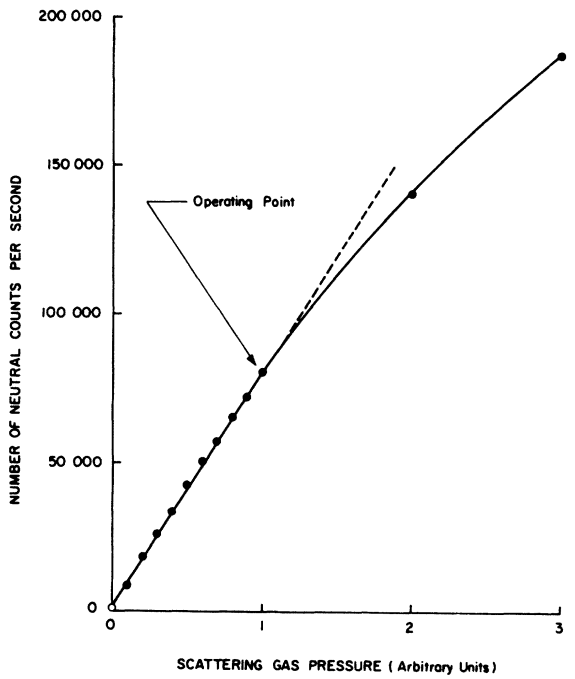

FIG. 2. Plot of He count rate as a function of scattering gas pressure. The figure shows the He signal reaching the detector at 0° in the 2.00-keV $He^+ + Ne \rightarrow He + Ne^+$ collision. All measurements are made in the linear region of the curve to ensure a predominance of single collisions. The small neutral-atom signal at zero pressure results from charge exchange of the incident ion beam with residual gas in the source and scattering chambers, as well as with various metal surfaces near the beam path.

Angular markings spaced at $\frac{1}{2}°$ intervals are etched on the edge of the circular stainless-steel table. When this scale is used in conjunction with a vernier mounted on the detector chamber, the angular position of this chamber is measureable in units of $\frac{1}{20}°$.

III. EXPERIMENTAL PROCEDURE

The experiments are performed by measuring the angular distributions of scattered He atoms arising from charge-exchange collisions, as well as the angular distributions of the combined He^+ and He signal.[2] Before making any measurements, it is important to determine a satisfactory operating pressure for each separate ion-atom pair to ensure a predominance of single collisions. In the present experiments, this is accomplished by measuring the count rate for neutral particles reaching the detector at 0° as a function of scattering gas pressure. Figure 2 shows a typical plot from the $He^+ + Ne$ experiment. It should be noted that only ballast-tank pressures are measured (via an ion gauge), and since they are neither absolute nor applicable to any other apparatus they are reported in arbitrary units. The operating pressure is selected in the linear region of the count-rate–versus–pressure curve. From the plot one notices a small neutral background beam at zero pressure in the scattering chamber. This results from charge exchange of the incoming ion beam with residual gas in both the source and scattering chambers, as well as with the various metal surfaces near the beam path. In all experiments, the maximum background neutral-atom signal is less than 2% of the charge-exchange signal in the forward direction.

Data are taken from 1.00 to 3.00 keV at 125-eV intervals in the $He^+ + He$ experiment and at 250-eV intervals in the $He^+ + Ne$ experiment. Data for the $He^+ + Kr$ experiment are taken at 1.00 and 3.00 keV. Angular data are taken at $\frac{1}{20}°$ intervals in the range from about 3 to $-1°$. The zero position of the beam is determined from the symmetry in the scattering pattern. A minimum of 200 particles are counted (per run) at each angular position to allow for statistical fluctuations in the count rate at the larger angles. A minimum of four angular runs are made at each energy. The data consist of both neutral-atom signals and combined neutral-atom and ion signals. The neutral-atom signal is recorded through 0°, while the combined data are recorded to a minimum angle of $\pm \frac{1}{2}°$, since inside this angle the incident ion beam may produce charged surfaces which affect the scattered ion signal.

In all experiments, the total number of scattered particles is counted at each angle by grounding both plates of the electrostatic analyzer. When a 500-V potential is placed on the lower plate, the charged

particles are deflected away from the detector and only the neutral particles are counted. The difference in counts is attributed to charged particles. In both the $He^+ + He$ and $He^+ + Ne$ experiments, the multiplier is adjusted relative to the electrostatic analyzer to permit direct detection of ions. Reversing the polarity of the analyzer voltage allows a search to be made for negative ions. The results of such measurements show that the only charged particles present in sufficient quantity to be distinctly distinguishable from the background signal are those of the He^+ variety. In addition, the number of He^+ particles detected in a given time interval compares very favorably to the difference between the total count (the total signal detected with both analyzer plates grounded) and the neutral atom count. This correlation was checked in both the $He^+ + He$ and in the $He^+ + Ne$ experiments at various energies and angles.

The variable of particular interest in these experiments is the charge-exchange probability $P_0(\theta, E)$, and its relationship to scattering angle and incident ion energy.[3] The charge exchange probability is defined as

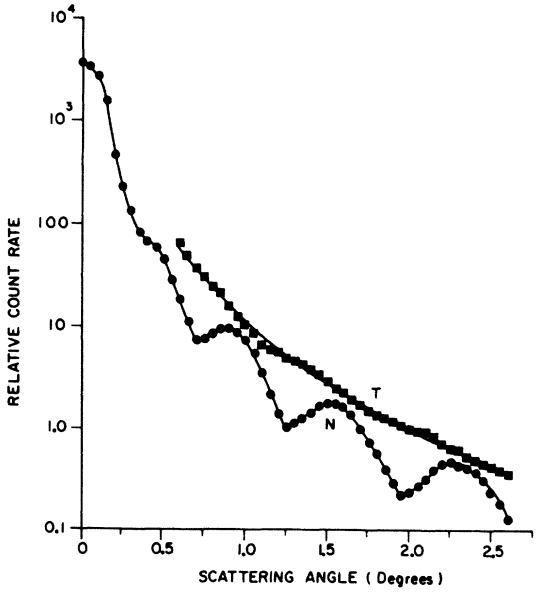

FIG. 3. $He^+ + He$ collision at an incident beam energy of 1.00 keV. The curve labeled N shows the relative count rate of the detected neutral He versus angular position of the detector, while curve T represents the relative count rate of all the He particles regardless of charge state. The data are normalized with respect to the neutral-atom data point at 3.00 keV and 1.50°. An interesting feature of curve T is the presence of a subtle oscillatory structure. This structure is interpreted as originating in the different detection efficiencies of the neutral atom and ion. Results for curve T are not shown for angles below 0.50°, since the incident beam may influence the data in this angular region.

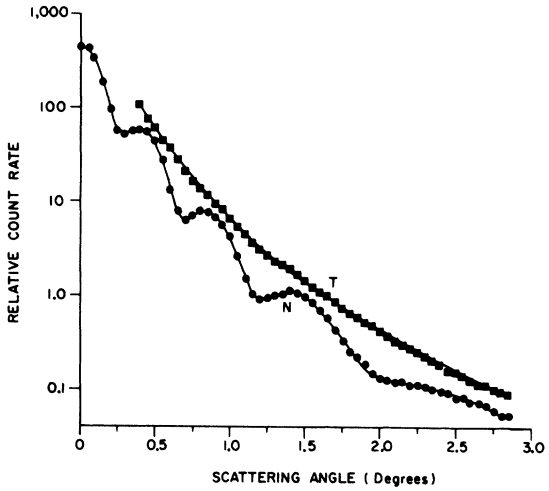

FIG. 4. $He^+ + He$ collision at an incident beam energy at 3.00 keV. The curve labeled N shows the relative count rate of the detected neutral He signal versus angular position of the detector, while curve T represents the relative count rate of all the He particles regardless of charge state. In contrast to Fig. 3, curve T, essentially, does not display an oscillatory structure. At this energy, the detection efficiencies of the neutral atom and ion should be equal.

$$P_0(\theta, E) = N(\theta, E)/T(\theta, E), \tag{1}$$

where θ is the scattering angle, E the incident ion energy, N the count rate of detected neutral particles, and T the count rate of all detected particles.

Although the detector cannot distinguish between a forward scattered neutral target particle and an incident He^+ ion which is neutralized in a charge-exchange collision, the analysis of all the data is based on the assumption that the small-angle differential cross section for a charge-exchange collision is much greater than the corresponding cross section for a hard ("head-on") collision.[4,5]

It should be mentioned that the retarding-potential method is used to determine the energy spread of the incident ion beam. These measurements show the spread to be less than ± 6 eV at all energies.

Prior to taking data, the ion beam is monitored by the Faraday cup in the scattering chamber. No data are taken until the ion beam intensity is stable to better than 1% over a 30-min interval. A 2-h warm-up period is generally required to achieve the necessary stability.

IV. RESULTS AND ANALYSIS

A. $He^+ + He$

The experimental results of the $He^+ + He$ collision at 1.00 keV are shown in Fig. 3, while Fig. 4 shows the results at 3.00 keV. The curves labeled N represent the relative count rate of the detected neu-

tral He versus angular position of the detector. Similarly, the curves labeled T represent the relative count rate of all the He particles, regardless of their charge state, versus angular position of the detector. Each data point of N and T is the combined result of four or more measurements and is normalized with respect to the neutral-atom data point at 3.00 keV and 1.50°. Plots for the He^+ ions are not shown, since they may be obtained by subtracting the various data points on N from the corresponding data points on T.

The pronounced oscillatory structure exhibited by curves N in Figs. 3 and 4 is indicative of a resonant-charge-exchange process. These oscillations result primarily from the elastic charge-exchange collision

$$He^+(1s) + He(1s^2) \rightarrow He(1s^2) + He^+(1s),$$

which is a symmetric, resonant process and may be interpreted as an interference between a *gerade* and an *ungerade* scattering amplitude. These same undulations were observed by Lockwood, Helbig, and Everhart.[4-6]

In a theoretical investigation of the $He^+ + He$ collision, Bates and McCarrol[7,8] showed that the charge-exchange probability P_0 is given by

$$P_0 = \sin^2 \xi , \tag{2}$$

where

$$\xi = J(R_0)/2v\hbar - \beta(v, R_0), \tag{3}$$

$$J(R_0) = 2\int_{R_0}^{\infty} [E_g(R) - E_u(R)] \frac{R}{(R^2 - b^2)^{1/2}}\, dR. \tag{4}$$

In the above equations $\beta(v, R_0)$ is a phase-factor term, R represents the internuclear separation, R_0 is the distance of closest approach, b is the impact parameter, v is the initial velocity of the incident ion, and $E_g(R)$ and $E_u(R)$ are the energies of the *gerade* and *ungerade* states. Lichten,[9] in treating this collision, states that the energies of the diabatic *gerade* and *ungerade* states should be used in the above formulation rather than energies of the adiabatic states. Using the diabatic energies, Everhart[3] neglected the phase-factor term $\beta(v, R_0)$, and by means of the impact-parameter method calculated the charge-exchange probability as a function of energy and angle.

One of the consequences of the above theory is that the probability of charge exchange should oscillate between the limiting values of 0 and 1. The probability measurements presented in this paper, as well as those of Lockwood, Helbig, and Everhart[4-6] and the related measurements of Aberth and Lorents,[10] fail to agree with the theory in this respect. An attempt was made to explain this discrepancy by reasoning that inelastic processes, which are neglected in the above theory, contribute significantly to the experimental probability measurements. Marchi and Smith,[11] using an elastic scattering approach, showed that the probability for charge exchange is given by

$$P_0 = \frac{|f_g(\theta, E) - f_u(\theta, E)|^2}{|f_g(\theta, E) - f_u(\theta, E)|^2 + |f_g(\theta, E) + f_u(\theta, E)|^2}, \tag{5}$$

where $f_g(\theta, E)$ is the scattering amplitude of the *gerade* state and $f_u(\theta, E)$ is the scattering amplitude of the *ungerade* state. Furthermore, as Ref. 11 points out, unless $|f_g(\theta, E)| = |f_u(\theta, E)|$, the limiting values of the probability must be different from 0 and 1.

Figure 5 shows plots of the charge-exchange probability as a function of angle. The measurements reported here are shown as solid circles and continuous lines, while the data of Lockwood, Helbig, and Everhart[4-6] are represented by solid triangles and broken lines. A comparison of the measurements shows two areas of disagreement. The most serious disagreement is in the large discrepancy of the probability values at the extrema. The maxima reported by Lockwood[4] are consistently lower than those reported in the present measurement, while the minima are consistently higher. The origin of this discrepancy seems to be the difference in angular resolution used in the two measurements. In addition to reporting an angular resolution four times lower than the resolution used in the present measurement, the angular resolution used in Ref. 4 was defined by a slit-hole arrangement which is extremely angle dependent at very small angles, while the hole-hole arrangement used here is not. The other area of disagreement is in the location of several of the extrema and does not appear to be serious.

Figure 6 shows the location of peaks and valleys as a function of energy and angle. Also shown are the locations of the $n = 3$ and $n = 6$ peaks as calculated by Everhart.[3] A more recent calculation by Demkov and Murakhver,[12] in which the rotation of the internuclear line is considered and a phase factor $\beta = \pi$ is used, shows excellent agreement with Everhart's calculation in this range of energy and angle. The slight disagreement between theory and experiment seems to indicate that the phase factor β must indeed have a velocity dependence and/or an impact-parameter dependence as suggested by Bates and McCarrol.[7]

Everhart[3] and Smith, Marchi, and Dedrick[13] have shown that, for small angles, the impact parameter b is a function of the product θT, where θ is the laboratory scattering angle and T is the laboratory energy of the incident projectile. A plot of the probability versus the reciprocal velocity v^{-1} at constant θT is thus a plot at constant impact parameter. Since the probability of charge exchange is given by (2), and at small angles the impact parameter and

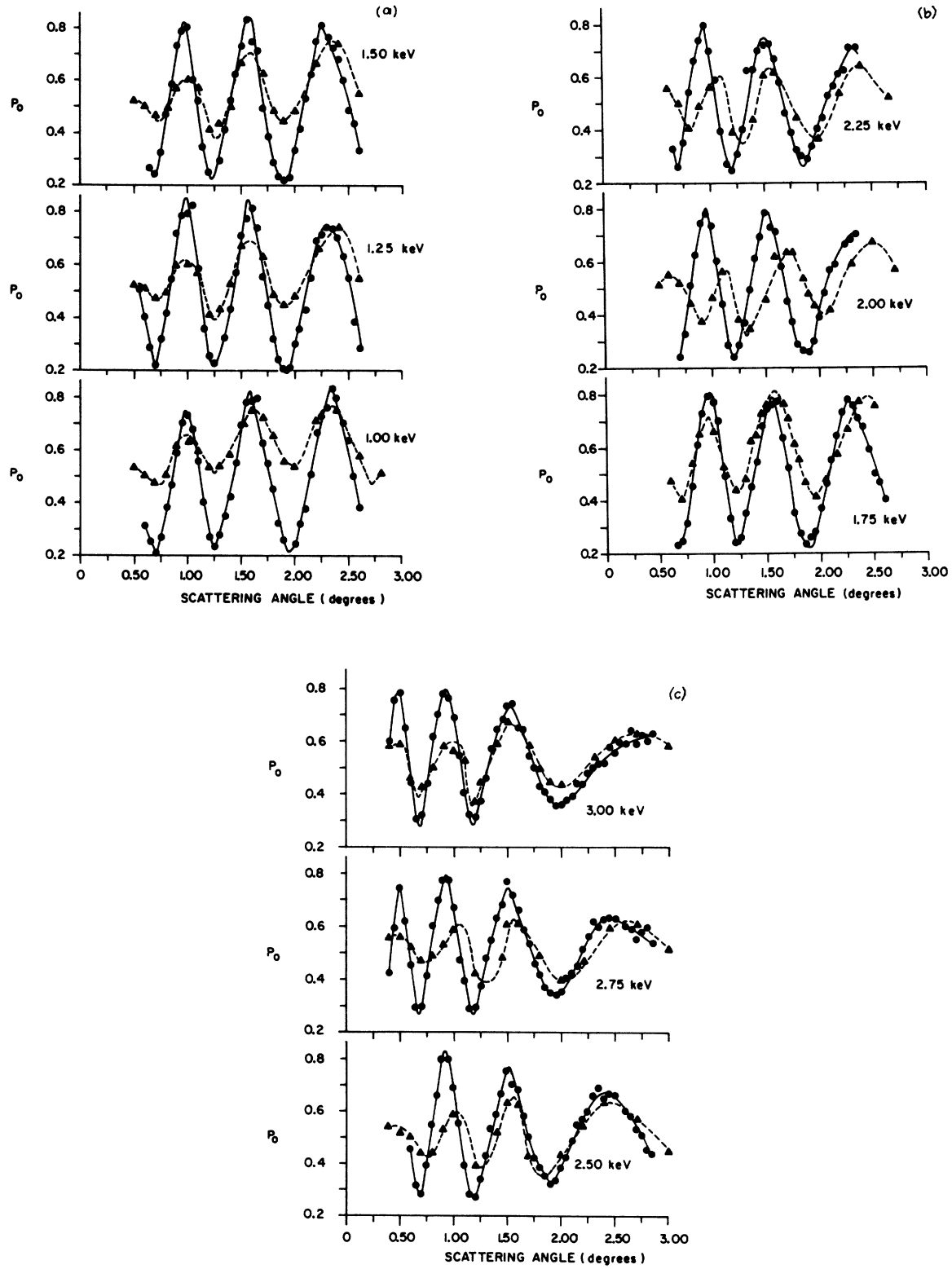

FIG. 5. Plots of the charge-exchange probability versus laboratory scattering angle for the $He^+ + He$ collision. The dashed curves show some of the results obtained in Ref. 4.

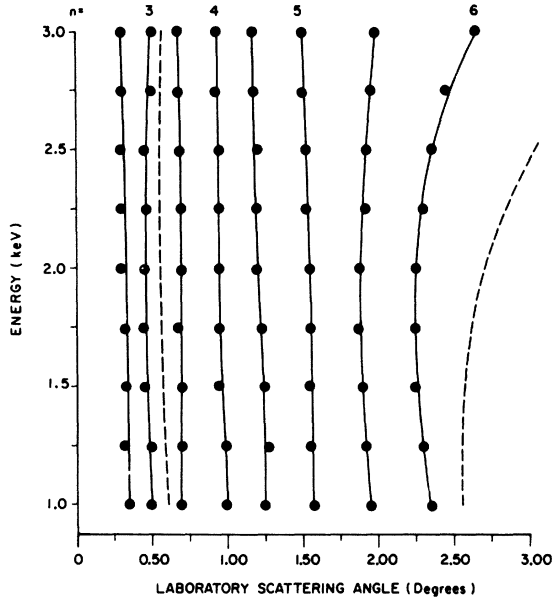

FIG. 6. Plot of the locations of maxima (integers) and minima in the charge-exchange probability as a function of energy and angle. The broken lines show the predictions of Ref. 3 for $n=3$ and $n=6$.

distance of closest approach are approximately equal ($b=R_0$), the locations of probability maxima are given by the expression

$$n-\tfrac{1}{2}=J(b)/hv-\beta(v,b)/\pi\,, \tag{6}$$

where $n=1, 2, 3, \ldots$ At constant θT (constant b), the distance between two adjacent peaks is given by

$$n''-n'=1=[J(b)/h]\ (1/v''-1/v') - (1/\pi)\,[\beta(v'',b)-\beta(v',b)]\,. \tag{7}$$

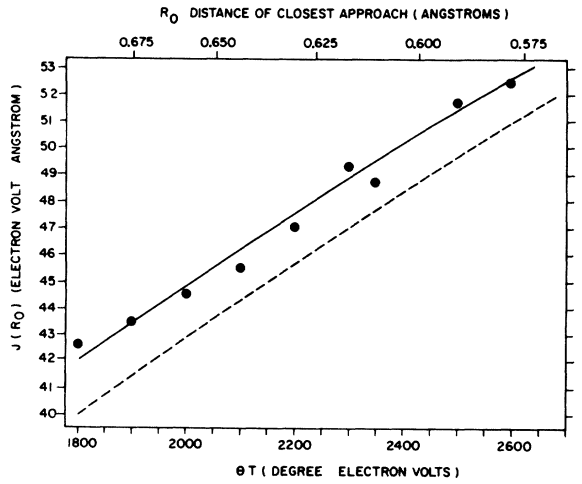

FIG. 7. Plot of $J(R_0)$ versus θT as obtained from the experimental data. The broken line shows results from Ref. 3.

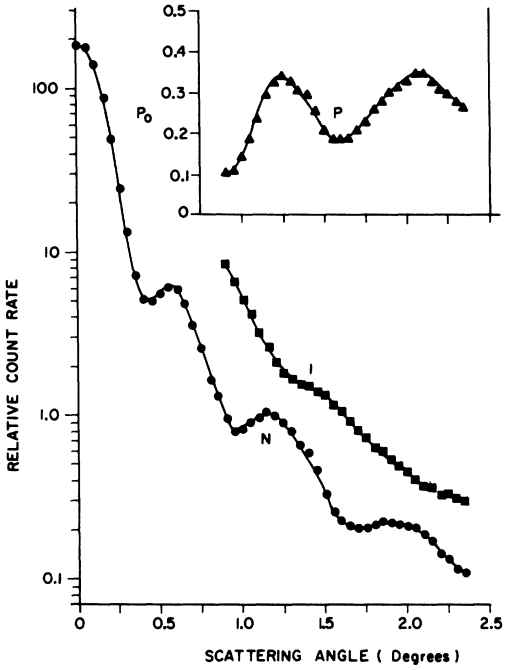

FIG. 8. $He^+ + Ne$ collision at an incident beam energy of 2.00 keV. Curve N shows the neutral He signal as a function of scattering angle, curve I shows the He^+ signal, and curve P represents the charge-exchange probability. Results for curves I and P are not shown for angles below 0.90°, since the incident beam may influence the data in this angular region. The data shown are normalized with respect to the neutral-atom data point at 3.00 keV and 1.00°.

A plot of the probability versus v^{-1} shows that the maxima and minima are evenly spaced. If we assume that $\beta(v'', b)=\beta(v', b)$, then we may obtain the value of $J(R_0)$ for several values of θT. Both the experimental values (solid circles and solid lines) and the values calculated by Everhart[3] are shown in Fig. 7. Although the values obtained from experimental data are consistently higher than the calculated values in the range shown, the agreement appears to be good.

An interesting feature of the curves labeled T in Figs. 3 and 4 is the presence of a subtle oscillatory structure. These oscillations are distinct in the 1.00-keV data of Fig. 3 and become less pronounced with increasing energy. Although the possibility exists that this structure is caused by inelastic channels, the authors believe that because of the location and period of these oscillations, a more reasonable interpretation is that the neutral-atom detection efficiency is not the same as the ion detection efficiency. Assuming this argument to be valid, a comparison of the smooth curve connecting the maxima to a similar curve connecting the minima indicates that, for the 1.00-keV data, the detection efficiency of a neutral helium atom is about

85% that of the ion. This, in effect, means that the values of the probability maxima for 1.00-keV data should be increased (by a small amount). This explanation of the subtle structure also suggests an experimental technique (discussed earlier) which may be used to obtain the ratio of the number of secondary electrons emitted by a surface as a result of neutral-atom bombardment to the number emitted by bombardment of the corresponding ion.

B. $He^+ + Ne$

The 2.00-keV $He^+ + Ne$ collision data shown in Fig. 8 are typical, in structure, of all the data taken at other energies for this collision. The curve labeled N is a plot of the relative count rate of the detected neutral particles versus the angular position of the detector, while the curves labeled I and P represent the relative count rate of the He^+ and the charge-exchange probability, respectively. All data obtained for this collision are normalized with respect to the neutral-atom data point at 3.00 keV and 1.00°. The results show an increase in the differential charge-exchange cross section (at 1.00°) with energy. Relative values of 0.59, 0.74, 0.84, 0.92, and 1.00 are obtained, respectively, for energies of 1.00, 1.50, 2.00, 2.50, and 3.00 keV. In contrast, the differential cross-section values for the ion signal decrease with energy having values of 7.23, 5.64, 5.02, 4.69, and 4.48 for the same energies. A plot of the charge-exchange probability as a function of angle is shown in Fig. 9. A most interesting result is that the locations of the maxima and minima in the probability curves are generally independent of energy. Similar measurements at higher energies gave values of P_0 which depend only on energy and not on scattering angle.[14] Such results are typical of resonant charge exchange, such as in the $He^+ + He$ case, and have been explained successfully by the use of a two-state approximation.

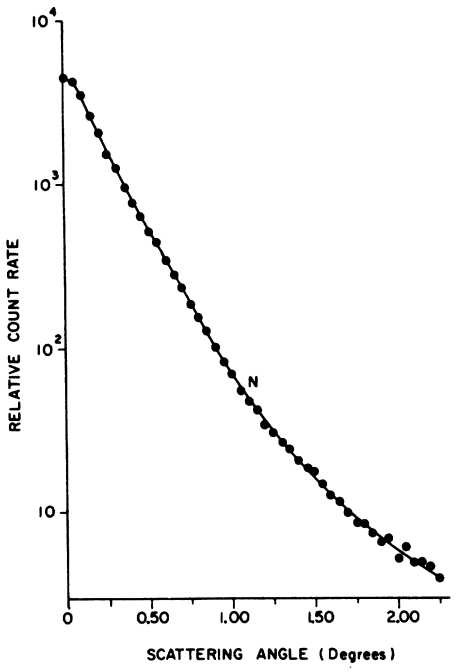

FIG. 10. $He^+ + Kr$ collision at 3.00 keV. The plot shows the relative count rate for He versus scattering angle.

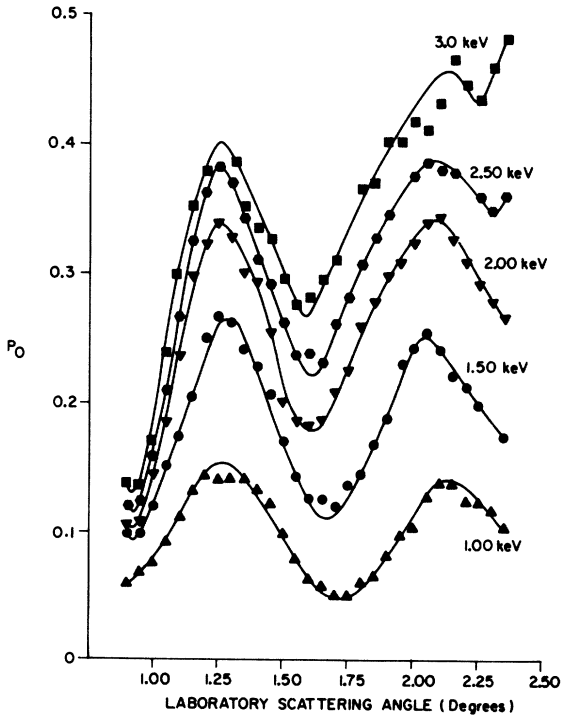

FIG. 9. Plots of the charge-exchange probability P_0 versus laboratory scattering angle for the $He^+ + Ne$ collision.

It is difficult to interpret these data in terms of a curve crossing and the resulting Stueckelberg oscillations,[15] since the observed forward scattering of the neutral atoms implies a crossing at a large impact parameter. Neither elastic nor inelastic[15,16] measurements on the $He^+ + Ne$ collision at lower energies indicate the existence of such a crossing. In addition, the locations of the Stueckelberg oscillations depend on expressions which are both energy and angle dependent.

The $He^+ + Ne$ charge-exchange collision may be classified as an asymmetric quasiresonant one. A theoretical model which describes this type of collision has been developed by Lichten.[17,18] The data are assumed to describe the collision $He^+ (1s) + Ne\ (2p^6) \rightarrow He\ (1s^2) + Ne^+\ (2p^5)$. At large separation, there is an energy defect of about 3 eV between the

$He^+(1s)+Ne(2p^6)$ and the $He(1s^2)+Ne^+(2p^5)$ systems. The adiabatic energies as a function of internuclear separation were calculated for this case by Michels,[19] and from these results the quality factor Q of the charge-exchange reaction,[17,18] may be estimated to be approximately 10, which according to this model is borderline between a resonant and a quasiresonant process.

In addition to the pronounced oscillations exhibited by the neutral-atom signal (N), a more subtle structure is observable in the ion signal (I). This structure becomes more evident with increasing energy, while a plot of the total signal (not shown) remains fairly smooth.

As Fig. 9 shows, the variation of the height of the probability curves is such that the maxima increase with increasing energy. This effect is in some ways similar to that found in the investigation[20] of the reaction $H^+ + He \rightarrow H + He^+$, and was interpreted[17,18] as a damping process.

The value of the integral $J(R_0)$ is determined for a value of $\theta T = 2.00$ keV deg, and is found to be approximately 46 eV Å. Lack of a greater range in energy and angle prevented a determination of $J(R_0)$ at other values of θT.

The authors feel that with increased angular resolution, or at lower energies, there should be a minimum in the forward-scattered neutral signal. It would be interesting to study the structure near the forward direction under these circumstances, as well as to determine definitely the final states of the colliding particles. Since the forward-scattered particles (in charge exchange) are neutral, these states can be best identified by a coincidence measurement.

C. $He^+ + Kr$

Preliminary data are taken at energies of 1.00 and 3.00 keV, with the latter shown in Fig. 10. In contrast to the previously discussed collisions, the most notable feature of these data is the lack of structure. Since the energy defect at infinite separation between the $He^+(1s)+Kr(4s^2, 4p^6)$ state and the $He(1s^2)+Kr^+(4s, 4p^6)$ state is only about 2.5 eV, one might expect a quasiresonant or resonant type of structure as was found in $He^+ + Ne$. Such is not the case, however, and these results are not understood at present. Here again a forward minimum in the neutral-atom signal may yet be found with increased angular resolution or at lower energies.

ACKNOWLEDGMENTS

The authors wish to thank Professor Edgar Everhart for the many fruitful discussions with him during the experiment. They also wish to thank W. J. Savola, Jr., and F. J. Eriksen for their assistance.

---

*Work supported by the Connecticut Research Commission, U. S. Army Research Office – Durham, and the University of Connecticut Research Foundation.

†From part of a thesis submitted by S. W. Nagy to the Graduate School of the University of Connecticut in partial fulfillment of the requirements for the Ph. D. degree, June, 1970.

‡Present address: Physics Dep't. University of Vermont, Burlington, Vt.

[1]S. W. Nagy, W. J. Savola, Jr., and E. Pollack, Phys. Rev. 177, 71 (1969).

[2]S. W. Nagy, S. M. Fernandez, and E. Pollack, in *Proceedings of the Sixth International Conference on the Physics of Electronic and Atomic Collisions* (M. I. T. Press, Cambridge, Mass., 1969), abstract of papers 867.

[3]E. Everhart, Phys. Rev. 132, 2083 (1963).

[4]G. J. Lockwood, doctoral thesis, University of Connecticut, 1964 (unpublished).

[5]G. J. Lockwood, H. F. Helbig, and E. Everhart, Phys. Rev. 132, 2078 (1963).

[6]E. Everhart, H. G. Helbig, and G. J. Lockwood, *Atomic Collisions Processes* (North-Holland, Amsterdam, 1964), p. 865.

[7]D. R. Bates and R. McCarrol, Proc. Roy. Soc. (London) A245, 175 (1958).

[8]D. R. Bates and R. McCarrol, Phil. Mag. Suppl. 11, 39 (1962).

[9]W. Lichten, Phys. Rev. 131, 229 (1963).

[10]W. Aberth and D. C. Lorents, Phys. Rev. 139, 1017 (1965).

[11]R. P. Marchi and F. T. Smith, Phys. Rev. 139, 1025 (1965).

[12]Y. N. Demkov and Y. E. Murakhver, in *Proceedings of the Fifth International Conference on the Physics of Electronic and Atomic Collisions* (Science Bookcrafters, New York, 1965), abstract of papers 132.

[13]F. T. Smith, R. P. Marchi, and K. G. Dedrick, Phys. Rev. 150, 79 (1966).

[14]E. N. Fuls, P. R. Jones, F. P. Ziemba, and E. Everhart, Phys. Rev. 107, 704 (1957).

[15]Dewitt Coffey, Jr., D. C. Lorents, and F. T. Smith, Phys. Rev. 187, 201 (1969).

[16]F. T. Smith, R. P. Marchi, W. Aberth, and D. C. Lorents, Phys. Rev. 161, 31 (1967).

[17]W. Lichten, Phys. Rev. 139, 27 (1965).

[18]W. Lichten, *Advances in Chemical Physics Vol. XIII* (Interscience, New York, 1967), p. 41.

[19]H. H. Michels (private communication).

[20]H. F. Helbig and E. Everhart, Phys. Rev. 136, 674 (1964).